

Calibrating Pan-Tilt Cameras in Robot Hand-Eye Systems Using a Single Point

Chandra Sekhar Gatla, Ron Lumia, John Wood, Greg Starr

Abstract—This paper describes a method that requires only a single projected point to calibrate a pair of cameras attached to pan-tilt units (PTUs) in a hand-eye robot configuration. Most existing calibration methods require either a set of known calibration locations or a large number of corresponding image features. These requirements usually imply human intervention, which complicates the calibration procedure. Rather than using multiple points in the workspace, the proposed algorithm uses a single stationary point generated by aiming a laser at a planar surface for the entire calibration. The single point provides a high intensity feature that is easy to extract from the image. To exercise all of the PTU and camera degrees of freedom, a large number of random robot/PTU configurations are computed automatically and 60 configurations, where both cameras can extract the single calibration point, are retained. As a result, this approach minimizes image processing requirements and virtually eliminates the correspondence problem. Using the Levenberg-Marquardt non-linear minimization algorithm, the Denavit-Hartenberg (D-H) parameters for the pan-tilt axes along with the internal and external parameters of the cameras are computed. This method requires no human intervention, employs simple image processing to detect the high intensity laser point, and produces a triangulation error of roughly 3mm at a range of 1 m.

Index Terms – Biclips, Camera Calibration, Pan Tilt cameras.

I. INTRODUCTION

CAMERA calibration is the process of determining the relation between the 3D coordinates of points in the workspace and their 2D image locations. The calibration includes internal and external parameters of the camera. Calibration of internal parameters finds the relationship between image coordinates and ray directions in the camera coordinate system. This relationship is described by the perspective projection of the perfect pinhole model. The parameters which need to be determined are the focal length, the principal point (image center pixel) and scale factors in the x and y directions. It is possible to include compensation

for lens distortion when a more accurate model is desired. Calibration of external parameters involves finding the position and orientation of the camera in some world coordinate system. External camera calibration is important in stereo vision where one needs to find the relative position of the coordinate systems of the two cameras and it is also important in hand-eye coordination in robots. Introducing pan-tilt motion to the cameras makes the external calibration dependent on the values of the pan and tilt angles. The calibration problem is to identify the values of the internal and external parameters of each camera in a stereo pair so that they can work together effectively, e.g., to determine 3D points of interest through triangulation.

II. RELATED WORK

Machine vision camera systems need quick, simple, easy and repeatable calibration methods. Many approaches to camera calibration exist. Some of these methods use a set of calibration points with known world coordinates. These world points can be obtained by either using a calibration object [1] in a known location or points marked in the workspace whose locations are measured. For example, a planar object with feature points clearly marked in a grid can be placed at a known location and moved by a known motion. Given this set of feature points with known world coordinates (X_i, Y_i, Z_i) and their projected locations in an image plane (u_i, v_i) , the external and internal parameters are found which will best map the world points to their image points by determining the parameters which minimize the mean square distance between the observed and computed positions of a feature on the image plane.

Other methods use geometric properties to calibrate cameras. These methods calibrate some of the internal camera parameters using invariant characteristics of geometric objects and their images. These methods do not require the position of the object relative to the camera. The aspect ratio is found using the image of a sphere [8]. Spheres are also used to locate the principal point [7]. The vanishing points [4] of parallel lines drawn on the faces of a cube are used to compute the principal point and focal length.

Some methods use only feature coordinates in the image plane to calibrate. These methods are called self calibration methods [2, 3, 9, 10] because they do not require known calibration points. It requires camera motion to take multiple images. Faugeras et al. [2] developed a method where a motion sequence of a single camera moving in an unconstrained manner can be used to calculate the internal

Manuscript received October 20, 2006 This work was supported in part by the U.S. Department of Energy under Grant # DE-FG52-04NA25590, issued to the University of New Mexico, Manufacturing Engineering Program.

Chandra Sekhar Gatla is with the Department of Mechanical Engineering, University of New Mexico, Albuquerque, NM 87131.

Ron Lumia is with Department of Mechanical Engineering, University of New Mexico, Albuquerque, NM 87131 USA (phone: 505-272-7155; fax: 505-272-7152; e-mail: lumia@unm.edu).

John Wood and Greg Starr are with Department of Mechanical Engineering, University of New Mexico, Albuquerque, NM 87131 USA (e-mail: {jw|starr}@unm.edu).

camera parameters. This method does not require known world coordinates of the calibration points. It requires only feature correspondences from a set of images where the camera has undergone pure rotation. In this method, the internal parameters of the camera are determined including radial lens distortion.

Calibrating a camera mounted on a pan-tilt mechanism involves the added effort of finding the location of the pan and tilt axes of rotation. Most of the existing methods of calibrating pan-tilt cameras have assumed PTUs with orthogonal axes, or have assumed a relatively simple geometric model of motion, in which axes of rotation are orthogonal and aligned with the camera imaging optics [11, 12, 13]. While this simplification works well over small volumes, accuracy suffers in a larger workspace, i.e., the camera model does not predict well the projection of a 3D feature point. In [6] a more complete model of pan-tilt cameras was employed, making the calibration suitable for use with low cost pan-tilt mechanisms. This method uses an existing tracking system consisting of stationary calibrated cameras. An LED point feature in the workspace is tracked using the fixed cameras to build a virtual calibration object that is then used to calibrate the pan-tilt cameras.

Most of the existing methods require either a known set of calibrated world points or a large number of corresponding image features. Either of these requirements makes the calibration process complicated and slow because the data gathering process must be supervised for correctness. Even a few correspondence errors will reduce considerably the accuracy of the resulting model. This paper describes a simple method to calibrate cameras and their PTUs using a single unknown stationary world point as the calibration point. Note that the 3D location of the point is unknown at the start of the process, and is determined during the calibration procedure. The data acquisition process is very much simplified by using a single unknown stationary 3D point (with reasonable initial guess); the extra effort to acquire multiple points is eliminated. Furthermore, with a single point to detect, a faulty correspondence of a feature between two cameras can never occur. Consequently, it is possible to use a very general model for pan-tilt camera motion and minimize human effort, since feature correspondence is unnecessary, in the calibration process.

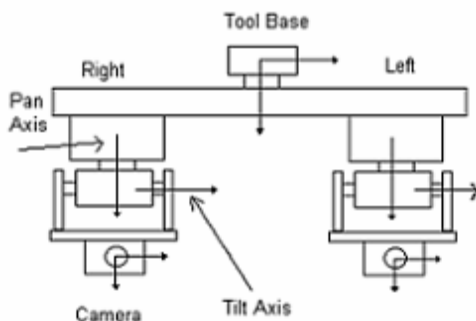


Fig 1. Biclops with Pan and Tilt Axis shown.



Fig 2. Staubli RX-130 robot carrying Biclops.

III. BICLOPS MODEL AND PARAMETERS

The camera system we used to acquire images of the workspace is called Biclops. Biclops is a custom-made, dual-camera motorized vision system. It consists of two FireWire color cameras, each attached to a pan-tilt unit (PTU). The PTUs are attached to a bracket, which is connected to a tool base as shown in Fig. 1. The robot picks up Biclops by connecting to the tool base as shown in Fig. 2. Biclops has four degrees of freedom, i.e., one pan axis and one tilt axis for each camera. The PTUs can be programmed to move the cameras to aim at any desired location in the workspace.

A. Coordinate systems

Biclops is built using standard PTUs and a metal frame. Though the dimensions of all the pieces are “known” through design, their accuracy cannot be assumed. Hence we need to model Biclops to determine the dimensions empirically. The coordinate system at which the robot holds Biclops is the robot’s tool control frame (TCF) which is indicated as frame E in Fig 3. We have defined D-H parameters for the two joints of each PTU. A coordinate frame is chosen on the CCD of the camera at the top left corner with the z axis out of the camera towards the objects,

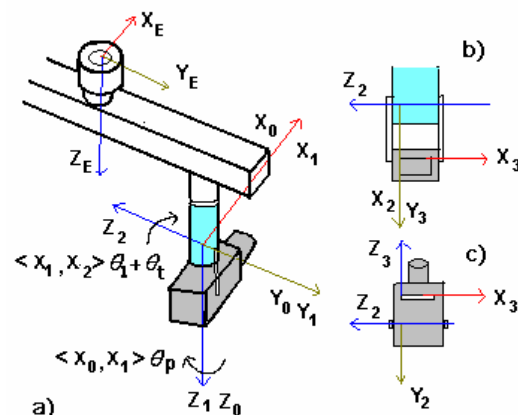


Fig 3. Biclops coordinate systems.

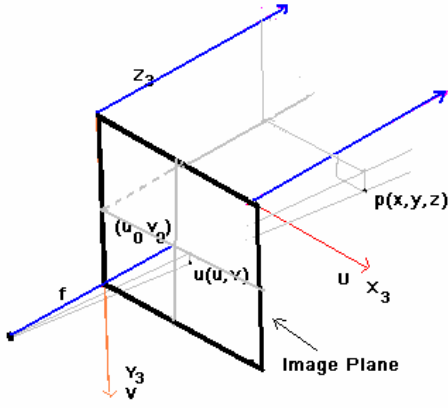


Fig 4. Image plane coordinate systems.

the x axis along the horizontal right direction, and y axis along the vertical down direction as shown in Fig. 4. All the coordinate frames are shown in Fig. 3. Fig. 4 shows the image plane coordinate systems with principal point (image center) (u_0, v_0) , focal length (f), and the projection of a 3D point $p(x, y, z)$ to (u, v) in camera coordinates. Although pan and tilt axes are shown intersecting and orthogonal in the Fig. 3 for clarity and simplicity, the model does not assume this. The separation and the angle between the pan and tilt axes are included in the D-H parameters that will be determined through the calibration procedure.

B. Transformation Matrices

The transformation matrices used to convert points from one coordinate frame to the next are given by the following equations. We use notation $c\theta_{12}$ for $\cos(\theta_1 + \theta_2)$, $s\theta_{12}$ for $\sin(\theta_1 + \theta_2)$ and ${}^A T_B$ for transformation matrix which transforms points described in frame B to points in frame A.

The transformation matrix from the base of the robot to the TCF frame is given by (1) as

$${}^B T_E = \begin{bmatrix} c\alpha c\beta c\gamma - s\alpha s\gamma & -c\alpha c\beta s\gamma - s\alpha c\gamma & c\alpha s\beta & x \\ s\alpha c\beta c\gamma + c\alpha s\gamma & -s\alpha c\beta s\gamma + c\alpha c\gamma & s\alpha s\beta & y \\ -s\beta c\gamma & s\beta s\gamma & c\beta & z \\ 0 & 0 & 0 & 1 \end{bmatrix} \quad (1)$$

where (x, y, z) is the position and α, β, γ are the yaw, pitch and roll rotation angles, respectively, of the TCF in robot base coordinate system. The transformation matrix from the TCF frame to frame 0 is given by (2),

$${}^E T_0 = \begin{bmatrix} c\theta_x c\theta_z & -c\theta_y s\theta_z & s\theta_y & t_x \\ s\theta_x s\theta_y c\theta_z + c\theta_x s\theta_z & -s\theta_x s\theta_y s\theta_z + c\theta_x c\theta_z & -s\theta_x c\theta_y & t_y \\ -c\theta_x s\theta_y c\theta_z + s\theta_x s\theta_z & c\theta_x s\theta_y s\theta_z + s\theta_x c\theta_z & c\theta_x c\theta_y & t_z \\ 0 & 0 & 0 & 1 \end{bmatrix} \quad (2)$$

where t_x, t_y , and t_z are the translation and θ_x, θ_y , and θ_z are x, y, z rotation parameters, respectively, from the TCF frame to frame 0. The other transformation matrices using D-H parameters are given by (3), (4) and (5),

$${}^0 T_1 = \begin{bmatrix} c\theta_p & -s\theta_p & 0 & 0 \\ s\theta_p & c\theta_p & 0 & 0 \\ 0 & 0 & 1 & 0 \\ 0 & 0 & 0 & 1 \end{bmatrix} \quad (3)$$

$${}^1 T_2 = \begin{bmatrix} c\theta_1 & -s\theta_1 & 0 & a_1 \\ c\alpha_1 s\theta_1 & c\alpha_1 c\theta_1 & -s\alpha_1 & -d_1 s\alpha_1 \\ s\alpha_1 s\theta_1 & s\alpha_1 c\theta_1 & c\alpha_1 & d_1 c\alpha_1 \\ 0 & 0 & 0 & 1 \end{bmatrix} \quad (4)$$

where θ_p is the pan angle and θ_t is the tilt angle. The D-H parameters from frame 1 to frame 2 are $\theta_1 + \theta_t, \alpha_1, a_1$ and d_1 . The angle between X_1 and X_2 is $\theta_1 + \theta_t$. The angle between Z_1 and Z_2 is α_1 , the separation between Z_1 and Z_2 along X_1 is a_1 , and the separation between X_1 and X_2 along Z_2 is d_1 .

$${}^2 T_3 = \begin{bmatrix} c\theta_2 & -s\theta_2 & 0 & a_2 \\ c\alpha_2 s\theta_2 & c\alpha_2 c\theta_2 & -s\alpha_2 & -d_2 s\alpha_2 \\ s\alpha_2 s\theta_2 & s\alpha_2 c\theta_2 & c\alpha_2 & d_2 c\alpha_2 \\ 0 & 0 & 0 & 1 \end{bmatrix} \quad (5)$$

where θ_2, α_2, a_2 and d_2 are D-H parameters from frame $OX_2 Y_2 Z_2$ to frame $OX_3 Y_3 Z_3$. The angle between X_2 and X_3 is θ_2 . The angle between Z_2 and Z_3 is α_2 . The separation between Z_2 and Z_3 along X_2 is a_2 . The separation between X_2 and X_3 along Z_3 is d_2 .

C. External Parameters

The transformation matrix which converts points from the base of the robot to a coordinate frame fixed on the camera is called the external transformation matrix. The external transformation matrix gives the location and orientation of the camera in the base coordinate frame of the robot (knowing the TCF position and orientation). The parameters of this external transformation matrix used in expressions (2) through (5) ($t_x, t_y, t_z, \theta_x, \theta_y, \theta_z, \theta_1, \alpha_1, a_1, d_1, \theta_2, \alpha_2, a_2, d_2$) are the external parameters.

D. Internal Parameters

The transformation matrix that converts points from the coordinate frame fixed on the camera to the 2D image coordinates is given by the following expression

$${}^I T_3 = \begin{bmatrix} fp_x & 0 & u_0 & 0 \\ 0 & fp_y & v_0 & 0 \\ 0 & 0 & 1 & f \end{bmatrix} \quad (6)$$

where f is the focal length, (u_0, v_0) is the location of the point where the axis of the camera intersects the image plane, i.e., the principal point. Parameters p_x, p_y are the number of pixels per mm (inverse scale factors) in the x and y directions, respectively, of the image. The parameters f, u_0, v_0, p_x and p_y are the internal parameters. This model does not include the lens distortion and the pixel skew, though the model can be easily extended to include them.

E. Calibration Matrix

The transformation matrix that transforms points from the base coordinate frame of the robot to the image coordinate frame is defined to be the calibration matrix, given by ${}^I T_B$.

$${}^I T_B = {}^I T_3 ({}^2 T_3)^{-1} ({}^1 T_2)^{-1} ({}^0 T_1)^{-1} ({}^E T_0)^{-1} ({}^B T_E)^{-1} \quad (7)$$

This matrix is clearly dependent on the values of the pan

and tilt axis angles because of 0T_1 and 1T_2 . 1T_B can be computed for any pan and tilt angles of a PTU if all the internal and external parameters are known. Given a 3D point X_B in the base coordinate frame of the robot, the calibration matrix is used to compute the location of the point in the image by $W = {}^1T_B X_B$. Vector $W = \{w_1 \ w_2 \ w_3\}^T$ contains the homogenous coordinates of the image point $U(u, v)$, computed by $u=w_1/w_3$, $v=w_2/w_3$.

IV. CALIBRATION

Calibration is the process of determining the values of all the parameters $\{t_x, t_y, t_z, \theta_x, \theta_y, \theta_z, \theta_1, \alpha_1, \alpha_2, \alpha_3, d_1, d_2, d_3, f, u_0, v_0, p_x, p_y\}$ of the model Φ . Given a point in the workspace, the corresponding image point can be computed using the values in Φ . The error between the computed and the observed points, as registered in the image plane, is called the projection error, and is the result of error in the estimation of the model parameters. Thus, choosing model parameter values that minimize the mean square projection error is the goal of the calibration procedure. This is described mathematically by (8):

$$\Phi_m = \underset{\Phi}{\text{Min}} \sum_{i=1}^n (U_i(\Phi, X_i, \theta_{pi}, \theta_{ti}, T_i) - \bar{U}_i)^2 \quad (8)$$

where \bar{U}_i is the observed image point and $U_i(\Phi, X_i, \theta_{pi}, \theta_{ti}, T_i)$ is the computed image point of the projected 3D point X_i in the base coordinate frame of the robot when the position of the end effector is T_i and pan and tilt values are θ_{pi} , and θ_{ti} respectively. In (8), $T_i = (x, y, z, \alpha, \beta, \gamma)$ is the set of translation and rotation values of the end effector, parameter ' n ' is the total number of 3D points observed, and Φ_m is the required parameter set that minimizes the mean square projection error.

To calibrate the model, the usual approach is to use a large set of 3D points and their corresponding 2D image points with respect to some pan, tilt angles and end effector position and orientation. The mean square of the projection error is minimized using Levenberg-Marquardt [5] nonlinear minimization. This procedure requires a known set of 3D points (X_i) in the workspace which are difficult to measure and time consuming to collect. The innovation of the proposed approach is that the calibration procedure herein is altered to use a single 3D point (X) and images of the point from various camera positions and orientations are taken. The modified calibration is represented by equation (9).

$$\Phi_m = \underset{\Phi}{\text{Min}} \sum_{i=1}^n (U_i(\Phi, X, \theta_{pi}, \theta_{ti}, T_i) - \bar{U}_i)^2 \quad (9)$$

The second distinguishing characteristic of the calibration procedure is to replace the known 3D point with an unknown but stationary 3D point in the workspace. The coordinates of the unknown 3D point are added to the set of calibration parameters to get a new set $\{\Phi, X\}$. The calibration procedure itself will determine the 3D location of the point (X). The final calibration is represented by equation (10),

$$\{\Phi, X\}_m = \underset{\{\Phi, X\}}{\text{Min}} \sum_{i=1}^n (U_i(\{\Phi, X\}, \theta_{pi}, \theta_{ti}, T_i) - \bar{U}_i)^2 \quad (10)$$

where X is the unknown stationary 3D point in the base coordinate frame of the robot. Using a single stationary 3D point does not affect the excitation of all the degrees of freedom of calibration as we still have the pan, tilt and the end effector location and orientation that can be varied extensively by moving the robot that carries Biclops.

V. EXPERIMENTS

A. Laser Pointer Tool

To determine that a calibration is accurate, an independent measurement must be made. To enable this, a laser pointer tool that can be attached to the robot wrist has been fabricated. It consists of a laser pointer (with pivot to adjust orientation) connected to a tool base. The robot picks up this tool by connecting to the tool base, as shown in Fig. 5. The robot can then aim the laser tool at any location in the workspace. This approach provides a simple but effective check on the calibration procedure. After the calibration procedure, the location of the calibration point can be computed and the laser pointing tool can overlay its laser point on the calibration point, thus verifying the results of the procedure.

B. Workcell

The workcell consists of two Staubli RX-130 robots, one carrying Biclops and the other carrying the laser tool, as shown in Fig. 6. These robots are on a robot transport unit (RTU) and can be moved along the track. An accurate calibration of the RTU system has been done which gives the transformation from the base of one robot to the other, measured experimentally to be within 1mm. The laser pointer aims at an arbitrary stationary location in the workspace. The robot carrying Biclops moves through a sequence of locations to exercise all of the degrees of freedom on the camera and PTUs. At each programmed location, the cameras on Biclops capture an image.



Fig 5. Staubli RX-130 robot carrying a laser pointer tool.

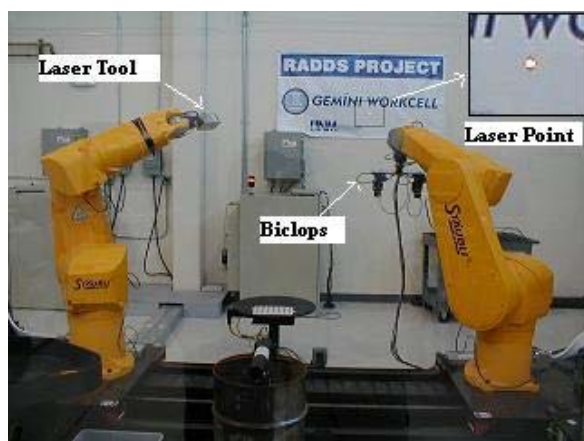


Fig 6. Workcell with two Staubli RX-130 robots on the RTU and laser point projected onto the wall .

C. Image acquisition and processing

The cameras on Biclops can be programmed for specific values of exposure time. Since the laser spot is quite bright relative to the other parts of the scene, a short exposure time ensures capturing only that spot. We assume that there are no other high intensity light sources in the workspace. This makes it very easy to process the images quickly to determine the location of the laser point in the images.

D. Procedure

The number of constraints required by the Levenberg-Marquardt algorithm to converge to a good model is usually five times the number of parameters in the model. Consequently, we used 60, 2D image points, which is equivalent to 120 constraints. Since the positions of the robot and values of the pan-tilt mechanism are under computer control, it is easy to ensure that each variable is exercised from minimum to maximum values. This persistent excitation prevents ill-conditioned matrices that result in poor models. The algorithm for the calibration procedure is as follows:

- 1) A laser pointer is aimed at an arbitrary location.
- 2) Random pan, tilt and TCF position and orientations are computed. This set is reduced to 60 positions, where the laser point is in the field of view of both cameras.
- 3) Biclops is moved by the robot to each of the set of positions and images of the laser point are captured.
- 4) These images are processed to determine the 2D coordinates of the laser point.
- 5) Once the data are collected for all positions the minimization routine (Levenberg-Marquardt) is used to determine the calibration parameters.

E. Results

Calibration of the pan-tilt cameras on Biclops requires only one unknown point to determine the values of the model parameters. Ideally, the same values of the model parameters should be obtained regardless of the location of the unknown point. In this section we repeat the calibration procedure of (10) using different unknown points to measure

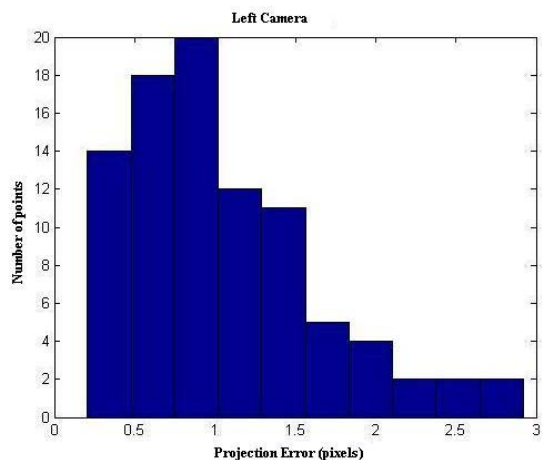


Fig 7. Histogram of the Projection errors for left camera.

the difference between the models obtained. Table I shows the 19 parameter values for each camera along with the obtained coordinates of the unknown stationary 3D point in two different trials using different unknown 3D points. An initial estimate of the parameters was determined from the “as designed” dimensions of the Biclops pan-tilt system. The Levenberg-Marquardt nonlinear minimization routine was used on the calibration data to compute values for the parameters that minimize the projection error. The model parameter values obtained from the two different unknown 3D points were within acceptable limits, as shown in Table I. For Trial 1, the “unknown” point was measured at (500, -

TABLE I
CALIBRATION PARAMETERS

Parameters	Trial I Point (500, -3198, 1368)		Trial II Point (700, -2148, 1254)	
	Left	Right	Left	Right
t_x (mm)	111.4615	-80.73 87	111.3205	-80.0354
t_y (mm)	-60.2324	122.68 54	-60.35	121.99 43
t_z (mm)	221.7315	230.9312	221.37	230.2173
θ_x (deg)	0.0592	0.1125	0.0761	0.0925
θ_y (deg)	-0.0854	-0.2831	-0.0732	-0.2478
θ_z (deg)	45.7232	45.5747	45.9421	45.0732
α_1 (deg)	90.2854	90.3832	90.5531	90.2987
a_1 (mm)	-8.9323	-9.5688	-9.0615	-9.8233
θ_1 (deg)	88.1076	86.7735	87.9864	86.1378
d_1 (mm)	9.8212	10.1115	9.5616	10.4156
α_2 (deg)	89.9718	90.2965	90.0515	90.3193
a_2 (mm)	54.1533	44.8755	54.3460	44.8043
θ_2 (deg)	-90.0723	-90.6572	-90.1289	-90.0667
d_2 (mm)	42.7024	27.9636	42.5957	27.5537
f (mm)	12.2565	11.9414	12.17111	11.9871
u_0 (pxls)	322.4034	333.5779	323.10	334.1599
v_0 (pxls)	260.584	264.3231	259.6133	265.1217
p_x (pxls /mm)	101.0467	101.4207	100.9734	101.8278
p_y (pxls /mm)	101.0243	100.2475	100.9958	100.0450
3D-X (mm)	499.297	498.265	700.325	699.654
3D-Y (mm)	-3197.035	-3196.214	-2148.014	-2147.092
3D-Z (mm)	1368.093	1367.215	1254.032	1253.256

3198, 1368). The computed values for the left and right cameras, the last three parameters in the model, show very small errors. Similarly, for Trial II, where the “unknown”

point was measured to be (700, -2148, 1254), the last three parameters in the model also show small error, certainly acceptable from the standpoint of grasping an object.

The calibration process was repeated in a similar fashion 90 times to test the accuracy of the calibration. The histogram of the projection error for the set of points was plotted as shown in Fig. 7 and Fig. 8. The projection error had range [0.5 to 2.8] pixels and mean close to 1 pixel.

Using the model computed for each camera and triangulating to a point 1000 mm away, a 1 pixel error creates an error of 3 mm. The time required for the complete calibration procedure is limited by the speed of the motion of the robot and PTUs. The procedure takes about three minutes to run. This compares favorably with the 20 to 30 minutes required for our previous calibration procedure that used a multi-point calibration grid. We are unaware of published calibration times for alternative approaches. Calibration using a grid requires more complex image processing and human involvement to verify the correctness of the corresponding image point locations; these problems were eliminated completely in the present method.

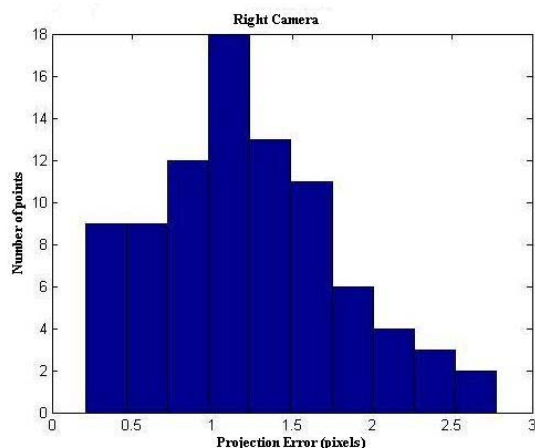


Fig 8. Histogram of the Projection errors for right camera.

VI. CONCLUSIONS

A novel method is developed to calibrate a pair of cameras mounted on PTUs where a pair of cameras analyzes images from a single fixed point in space. The correspondence problem has been eliminated completely, and image processing has been simplified to finding the only bright dot in an image.

A complete model without any assumptions about the PTU geometry is considered. The present method does not require either an extensive set (or any, for that matter) of known calibration points in the workspace or an expensive routine to make the image features correspondences.

A single unknown stationary 3D point in the workspace, designated by aiming a laser pointer at some surface in the workspace, is sufficient to derive the vision system model parameters. The values of robot location, pan,

and tilt can be generated automatically using inverse kinematics (with initial approximation of the parameters) so that the algorithm can run unattended whenever needed.

ACKNOWLEDGMENT

This work was supported by DOE Grant # DE-FG52-04NA25590, issued to the University of New Mexico (UNM) Manufacturing Engineering Program. We would also like to thank Dave Vick and Colin Selleck who helped the authors with the experiments on the Staubli RX-130 robots.

REFERENCES

- [1] R. K. Lenz and R. Y. Tsai, "Techniques for calibration of the scale factor and image center for high accuracy 3D machine vision metrology," in *IEEE Trans. on Pattern Analysis and Machine Intelligence*, vol. 10, no. 5, pp. 713-720, Sept. 1988.
- [2] O.D. Faugeras, Q.T. Luong, and S. J. Maybank, "Camera Self-Calibration : Theory and Experiments," In *Proceedings of the Second European Conference on Computer Vision*, pp. 321-334, Santa Margherita Ligure, Italy, May. 1992.
- [3] Q. T. Luong and O. D. Faugeras, "Self-calibration of a moving camera from point correspondences and fundamental matrices," *International Journal of Computer Vision*, vol. 22, no. 3, pp. 261-289, 1997.
- [4] B. Caprile and V. Torre, "Using vanishing points for camera calibration," *Int. Journal of Computer Vision*, vol. 4, no. 2, pp. 127-140, March 1990.
- [5] J. J. Mor'e, "The Levenberg-Marquardt Algorithm: Implementation and Theory," *Numerical Analysis, Lecture Notes in Mathematics*, Springer Verlag, Vol. 630, pp. 105-116, 1977.
- [6] J. Davis and X. Chen, "Calibrating pan-tilt cameras in wide-area surveillance networks," In *Proc. of ICCV 2003*, Vol 1, pp. 144-150, October 2003.
- [7] Guruprasad Shivaram, Guna Seetharaman, "A New Technique for Finding the Optical Center of Cameras," *ICIP*, vol. 2, pp. 167-171, 1998.
- [8] M. Penna, "Camera Calibration: A Quick and Easy Way to Determine the Scale Factor," in *IEEE Trans. Pattern Anal. Machine Intelligence*, vol. 12, no. 12, pp. 1240-1245, 1991.
- [9] R. Hartley, "Self-calibration from multiple views with a rotating camera," In *Proc. Third European Conf. on Computer Vision*, pp. 471-478, 1994.
- [10] S.J. Maybank and O.D. Faugeras, "A Theory of Self Calibration of a Moving Camera," *Int'l Journal of Computer Vision*, vol. 8, no. 2, pp. 123-151, 1992.
- [11] D. C. Woo and D. W. Capson, "3D visual tracking using a network of low cost pan/tilt cameras," presented at *Canadian Conference on Electrical and Computer Engineering Conference Proceedings*, 2000.
- [12] A. Basu and K. Ravi, "Active camera calibration using pan, tilt and roll," *IEEE Transactions on Systems, Man and Cybernetics, Part B (Cybernetics)*, vol. 27, pp. 559-66, 1997.
- [13] S. Fry, M. Bichsel, P. Muller, and D. Robert, "Tracking of flying insects using pan-tilt cameras," *Journal of Neuroscience Methods*, vol. 101, pp. 59-67, 2000.